Modelling and Measurement Results for RF Power amplifiers characterization with Memory effects

Chokri Jebali[1], Ghalid Idir Abib[2], Ali Gharsallah[1] and Eric Bergeault[2]

[1] Laboratoire d'Electronique, Facultés des Sciences de Tunis, 2092 El Manar Tunisia
[2] Laboratoire Radiofréquences et Micro-ondes, Département COMELEC,
Ecole National Supérieure des Télécommunications (ENST Paris), 46 rue Barrault, 75634 Paris Cedex 13, France
jebalichokri@yahoo.fr

Abstract:
In this paper, the experimental and the modelling investigation of nonlinear RF power amplifier are presented. A cross-covariance calculation was firstly being applied to the raw signals sampled at the Device Under Test (DUT) input and output to cancel the time delay. The behavioural polynomial model used to assess the system identification is characterized by the Normalized Mean Square Error (NMSE). These measurements are performed on a GaAs MESFET power transistor operating in class AB, driven by QPSK signal at 1575MHz. To accurately identify the memory effects, a time delay estimation study based on cross-covariance and Lagrange interpolation, was used to align the input and output raw baseband data. The results show a good agreement between measurement, conventional polynomial model, and the orthogonal polynomial model.

Key words- power amplifier, polynomial model, orthogonal basis, memory effects, numerical stability

I. INTRODUCTION

The cellular revolution is the significant reason in the growth of the mobile phone market. The first generation wireless phones used analog devices technology, although their inconvenient they demonstrated successfully their flexibility with mobile communications system [1]. The actual wireless generation systems are built using digital devices technology. The digital system provide much more traffic, better reception quality and security level compared to the analog systems [1]-[4]. The current wireless generation can deliver a wide variety of services by access to the internet services in which can upload high information rates for different frequency ranges. For the next generation wireless devices, development effort in digital technologies makes use of higher frequencies to increase capacity of support. The signal intensity of an analog signal varies in a smooth level over time without any discontinuities compared to the digital signal intensity which keep a constant level for some time period then changes to another level. Indeed, the two terms continuous and discrete correspond to analog and digital are often used in data communications such as, data transmission and signals [5].

In general, any amplifier, when driven into a strong nonlinear condition, will generate amplitude and phase distortion [6]. This is characterized by the amplitude modulation conversion (AM-AM) and phase modulation conversion (AM-PM) which represents a variation in the phase and the amplitude of the transfer characteristic as the power amplifier output level becomes near the compression point [7]. The spectrum resulting from nonlinear amplification has a stepped appearance, with each step corresponding to a higher order of distortion [8]. These steps are known as spectral regrowth sidebands or adjacent channel power (ACP) [9]. Intermodulation distortion (IM), or spectral regrowth are considered as the mainly problem of adjacent channel interference [10], indeed, transmitter power amplifier (PA) linearity is often specified in terms of demodulation error rates, rather than ACSR (adjacent channel spectral regrowth)[11].

There are some standard issues that affect the operation and design of any nonlinear power amplifier such as standard modulation formats encountered in wireless communications systems. The more used modulation format is the $\pi/4$ DQPSK used in the North American Digital Cellular system (NADC), which present a compromise between the high channel capacity and low envelope amplitude variation. As mentioned in the literature[12][13], it is possible to employ the same envelope approach to estimate the distortion levels in the RF power amplifier PA to well analyse any modulation formats. Mobile radio systems interest are fixed around other types of modulation such as quadrature amplitude modulation (QAM), the quadrature phase shift keying (QPSK), and the 16-QAM for mobile radio systems. The use of linear modulation format in mobile devices often requires a highly linear amplification, therefore, the major reason for employing a linear scheme i.e. narrow channel bandwidth is the spectrum efficiency. Some systems require the use of multiple channels simultaneously such as on travelling wave tube amplifiers (TWTAs) [14].

The multicarrier transmitters using a multiple narrow band carriers for transmitting a high bit rate data without require for an equalizer. The modulation format used by this transmitter is the orthogonal frequency division multiplexing (OFDM) which involves many individual carriers in which everyone can be treated alone within the coherence bandwidth of the channel. The use of narrow band carriers in sufficient manner can remove the need for an equaliser [1].

The behavioural model of non linear power amplifier excited by a wide band WCDMA signal, suffer from accurate modelling approach. With a simple periodic signal, a WCDMA signal approximation is did, then, excited to the power amplifier PA device as an input, then, after deriving the AM/AM and AM/PM data characteristics and used them as the basis of the power amplifier PA behavioural model the AM/AM characteristics issue from a tapped delay-line (TDL) power amplifier PA model using linear filters is described [2]. Some high speed digital communication system needs the wide and ultra wide bandwidth modulation formats in which a linearization schemes (for analog and digital) is needed to pre-compensate the signal before the amplification [3]. Recent behavioural modelling approach for micro-wave non linear power amplifier using a Volterra series development is described [4]. The behavioural model of non linear power amplifier driven by a wideband signal using a memoryless model suffers from memory effect. Therefore, the need to use another models such as V-vector Volterra and memory polynomial model with sparse delay (MPMSD) able to model the memory effects [15].

In this paper, we suggest an experimental testbed to carry out the input output data in which we characterize a behavioural polynomial model for nonlinear power amplifier when cancelling the time delay to reach predistortion taking account with memory effects for a significant linearization.

The organisation of this paper starts in section II with an overview of theoretical approach of the behavioural model characterizing the transfer function of the DUT, the error and the cross-covariance technique. In section III, The description of the measurement system setup and the device under test (DUT). In section IV, the experimental and modelling results are presented to show the significant performances of our proposed study. Finally, conclusions are drawn in section V, which summarizes all the advantages of this study by giving some results recommendations.

II. THEORITICAL APPROACH

A general model for power amplifier behaviour is Volterra series; this model requires a wide number of basic functions. We applied in our work special cases of Volterra series [10], several polynomial based models have been studied. These are namely the envelope memory polynomial model, the conventional memory polynomial model, and the orthogonal memory polynomial model [11]. The input and output power amplifier measurements for an excited QPSK signal are used for these Polynomial models. The mathematical formulation of the conventional polynomial model is given by:

$$y(t)=\sum_{i=1}^{K} a_i x(t)\left|x(t)\right|^{i-1} \tag{1}$$

$$\tilde{y}_{MPM}(n)=\sum_{j=0}^{Q}\sum_{i=1}^{K} a_{ij}\cdot x(n-j)\cdot\left|x(n-j)\right|^{i-1} \tag{2}$$

Where x(n) is the input measurement, y(n) is the output measurement, k is the polynomial order, M is the memory depth, and a_{ij} are the polynomial coefficients. When the complex gain of the device under test is function of the magnitude of the input signal, we describe the envelope memory polynomial model with:

$$\tilde{y}_{EMPM}(n)=\sum_{j=0}^{Q}\sum_{i=1}^{K} a_{ij}\cdot x(n)\cdot\left|x(n-j)\right|^{i-1} \tag{3}$$

The orthogonal memory polynomial model uses a set of basis functions to significantly improve the identification accuracy by reducing the conditioning of the matrix to be inverted in the LS identification. The orthogonal model's output is described by:

$$\tilde{y}_{OMPM}(n)=\sum_{j=0}^{Q}\sum_{i=1}^{K} a_{ij}\cdot\sum_{l=1}^{i} U_{li}\cdot x(n-j)\cdot\left|x(n-j)\right|^{l-1} \tag{4}$$

where U_{li} is given by:

$$U_{li}=\begin{cases}(-1)^{l+i}\cdot\dfrac{(i+l)!}{(l-1)!(l+1)!(i-l)!} & \text{for } l\le i\\ 0 & \text{for } l>i\end{cases} \tag{5}$$

The identification of the polynomial coefficients is given by the Least Square Method (LS) in transforming equations to a matrix form. For the MPM, EMPM and OMPM models, it is possible to define a formulation as:

$$\Phi_{ji}(n)=\begin{cases}x(n-j)\cdot\left|x(n-j)\right|^{i-1} & \text{for the MPM model}\\ x(n)\cdot\left|x(n-j)\right|^{i-1} & \text{for the EMPM model}\\ \Psi_{ji} & \text{for the OMPM model}\end{cases} \tag{6}$$

Where the basis function of the orthogonal model is:

$$\Psi_{ji} = \sum_{l=1}^{i} U_{li} \cdot x(n-j) \cdot \left| x(n-j) \right|^{l-1} \quad (7)$$

$$A_{LS} = \left(\Phi^H \Phi \right)^{-1} \Phi^H y \quad (8)$$

In the orthogonal polynomial model, the basis Φ is referred by Ψ in the whole of the expressions.

$$\Phi_i(x(n)) = x(n) \left| x(n) \right|^{i-1} \quad (9)$$

$$y = [y(t_1), \ldots, y(t_n)]^T \quad (10)$$

$$x = [x(t_1), \ldots, x(t_n)]^T \quad (11)$$

$$\phi = [\phi_1(x), \ldots, \phi_k(x)] \quad (12)$$

$$\phi_k(x) = [\phi_k(x(t_1)), \ldots, \phi_k(x(t_n))]^T \quad (13)$$

Φ^H is the Hermitian transpose.

In equation (14), we add the influence of the memory effect introduced by thermal effect, aging and the influence of the wideband signal.

$$\tilde{y}(n) = \sum_{j=0}^{Q} \sum_{i=1}^{K} a_{ij} \cdot \Phi_{ij}(n) \quad (14)$$

Where k is the polynomial order, Q is the memory depth order, and a_{ij} are the polynomial coefficients.
The MPM, EMPM, and OMPM models described above were identified for the device under test under the QPSK signal. For all the considered models, the nonlinearity orders and memory depth were set to $K = 15$ and $Q = 4$ respectively. The matrix form of the orthogonal memory-less and memory polynomial model is given in [11].

Fig. 1, shows the function $\Phi_k(|x|) = |x|^k$ versus $|x|$, this figure provides that if $x \to 0$ (tends towards zero) the basis function $\Phi_k(x)$ of the conventional polynomial model tends towards zero faster than x for an order k superior of 1.

We can express $\Phi_k(x)$ with:

$$\Phi_k(x) = O(x^k) \quad (15)$$

$$\text{i.e. } \lim_{x \to 0} \left(\Phi_k(x) / x^k \right) = a \quad (16)$$

where the constant a satisfies $0 < |a| < \infty$

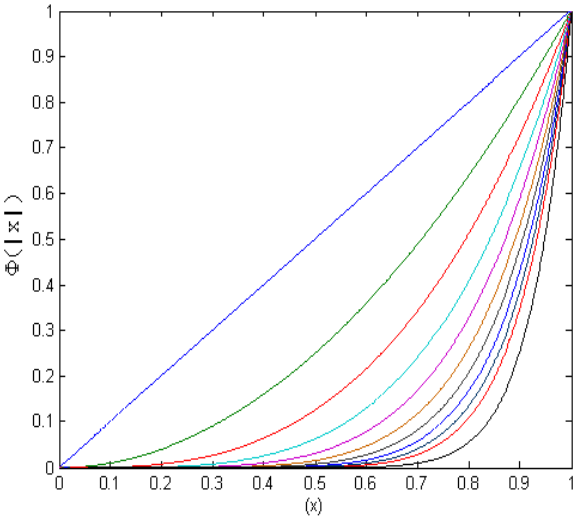

Fig.1. Conventional polynomial basis

The Behavioural Polynomial models can be applied with more accuracy when we compared their performances versus the output measurement data. To give a quantitative measure of the polynomial model accuracy, the Normalized Mean Square Error (NMSE) was used to assess the performance of the considered models.
The NMSE is given by:

$$NMSE \ (dB) = 10 \cdot \log_{10} \left[\frac{\sum_{n=1}^{N} \left| y(t_n) - \hat{y}(t_n) \right|^2}{\sum_{n=1}^{N} \left| y(t_n) \right|^2} \right] \quad (17)$$

Where N is the number of samples in the measured waveforms, y and $\tilde{y}$ are the measured and the estimated DUT output waveforms respectively.

Many techniques are described in the literature, but in our paper we applied cross-covariance technique to estimate the delay between the input and the output complex waveforms [7].

$$C_{xy}(n) = \begin{cases} \sum_{k=0}^{K-n-1} \left(x(k+n) - \bar{x} \right) \cdot \left(y^*(k) - \bar{y}^* \right) & \text{for } n \geq 0 \\ \sum_{k=0}^{K+n-1} \left(x^*(k-n) - \bar{x}^* \right) \cdot \left(y(k) - \bar{y} \right) & \text{for } n < 0 \end{cases} \quad (18)$$

The cross-covariance is described in equation (12), where $x(k)$ and $y(k)$ are respectively the input and output baseband waveforms, $\bar{x}$ and $\bar{y}$ are the mean values of x and y waveforms respectively, $x^*(k)$ and $y^*(k)$ denotes the complex conjugate of the sample

$x(k)$ and $y(k)$ respectively and K is the number of waveforms samples. n (resp. $n_{\max}$) is the value of the integer for which $C_{xy}(n)$ is maximal, the optimal delay expressed in number of samples where the absolute value of the delay in time units is given by:

$$\mu = \frac{1}{r \cdot f_s}.n_{\max} \quad (19)$$

Where r and f_s are respectively the up-sampling ratio and the original sampling frequency.

The time delay between the input and the output baseband data waveforms has to be accurately estimated. Indeed, the requirement to align input and output streams is prior than identifying the power amplifier model. In wideband, the time delay estimation is critical, because any time delay misalignment causes an extra dispersion of AM/AM and AM/PM characteristics of the power amplifier. The time delay estimation accuracy is mainly carry out by the sample rate f_s. Such example, if the sample rate f_s is more than 60 Msps, the time resolution is around 16 ns. Therefore, in practical, the time delay of a power amplifier is lower than 15 ns, where the resolution is larger than the time delay induces by the PA. Indeed, the sample rate is unable to carry out the requirement of time delay estimation and should be increased. Consequently, it is shown that the sample rate fully depends on the speed of the analog- to-digital converters (ADC). Due to the currently available ADC speed and the expenses, it seems difficult to circumvent this limitation. The alternative solution, is to use digital signal processing(DSP) techniques. In this work, the Lagrange interpolation [7], has been used to increase the sample rate by 20-30 times, then, a satisfactory time-delay estimation achieved and a higher resolution can be obtained.

The performance of the memory-less and the Memory Polynomial model of the Power Amplifier are illustrated. in the next section.

III. EXPERIMENTAL SETUP

We consider in this part, the description of the baseband measurement bed architecture and the real testbed in fig.2 and fig.3 respectively, which shows the complete architecture of the measurement system. Which contain the DUT (Device Under Test), the polarization, the filters and the generator RF source which can provide several RF modulation schemes signals. The measurement data are extracted from a GaAs MESFET Fujitsu FLL107ME transistor in which the static characteristics of the drain current versus the drain source voltage for different source grille voltage values are taken from [6].

The baseband measurement bed uses an ESG 4431B signal generator from Agilent Technologies. The ESG generator deliver a QPSK modulation format signal with 1 Msps of symbol rate and a 1.575GHz of central frequency. For a high output power, it is necessary to insert optimum impedance (Tuner) in the transistor output with a reflection coefficient equal to 0.4. The roll-off factor used in this measurement bed for the baseband digital Nyquist filter is equal to 0.35, the impedance at the harmonic frequencies ($2f_0$, $3f_0$) for the DUT input output are closed to 50 ohm using pass band filter and wide band circulator.

The polarization point corresponds for AB class's power amplifier operation. In table 1, the S parameters are presented for the MESFET transistor and for the polarization point.

Table 1: S parameters for a transistor Fujitsu FLL107ME with operation frequency 1.575GHz (Vgs = -1.7v, Vds = 10v, Ids = 44mA)

	S_{11}	S_{12}	S_{21}	S_{22}
Linear Module/(dB)	0.89/ -0.91	0.04/ -28	3.69/ 11.34	0.46/ -6.7
Phase[°]	-140	3.29	71	-89

The experimental bed is shown in fig.2 which contains passive and active elements; the proposal architecture aims to dynamically extract the input output data from the Device Under Test (DUT) implemented in the measurement bed.

The use of power amplifier characteristic is presented in the following subsection that is based on measurements. The simulations are performed with QPSK modulation using a square root cosine roll-off filter with roll-off factor 0.35 at the transmitter.

IV. RESULTS AND DISCUSSION

In previous literature, the description of the basis function implementation with a LUT can generate an error when a low input value is forced to zero caused by quantization. In equations (1) and (14) describing memory-less and memory conventional polynomial model, which suffered from a numerical instability problem associated with the basis function Φ. This instability is shown in fig. 4, by plotting the condition number of the square matrix $(\Phi^H \Phi)$ for two cases, the memory-less and the memory conventional Polynomial model, in which the order of the memory depth is equal to Q = 4, and the order of nonlinearity is K= 15. We note that, the condition number grows exponentially as soon

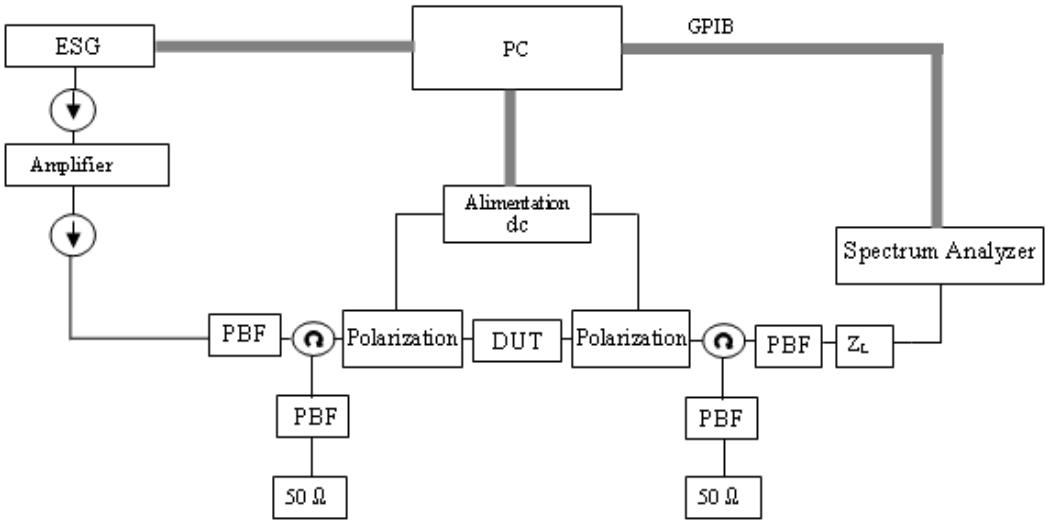

Fig.2. Block diagram of the experimental setup measurement test bed, transistor Fujitsu FLL107ME.

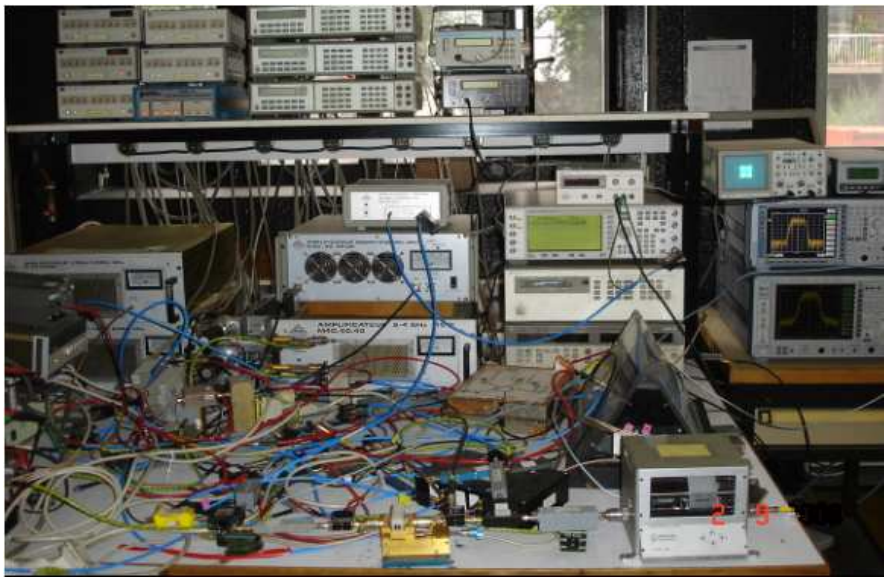

Fig.3. Test bed measurement section for the data (input and output) extraction and characterization

as the polynomial order and the delay tap increases for 3000 samples.

Our results demonstrate that Memory Polynomial models led to comparable performance in time domain and frequency domain. Indeed, the complexity and the identification robustness comparison of these models are given. It was carried out that for the same Device Under Test (DUT), driven by QPSK signal, the power series model and the Orthogonal Memory Polynomial model have the same parameters (nonlinearity order and memory depth). As can be seen, the models have the same number of coefficients and the same numbers of basis functions due to their similar formulation.

Indeed, the coefficients estimation of the models using input output samples data lead to numerical instability of the pseudo-inverse calculation. The result is inaccurate when finite precision calculation is needed. Centring algorithm and data scaling was applied to avoid the high condition numbers. Where the new input data depend on the mean value and the standard deviation of the signal, described by:

$$x'(n) = \frac{x(n) - \overline{x}}{\sigma_x} \tag{20}$$

Where σ_x : the standard deviation, and $\overline{x}$ the mean value of the input waveform.

However, to improve the conditioning of the pseudo-matrix for the orthogonal polynomial models, input signal normalization was used : $x'(n) = \dfrac{x(n)}{\max|x(n)|}$.

The result illustrates significant improvement achieved by pre-processing the input samples, while the relative

computational complexity evaluation. Furthermore, in fig. 5, the results carry out the lower condition number of the Orthogonal Polynomial model, and the robustness of the pseudo-inverse calculation compared by the others models, we note that the envelope memory polynomial model has the same behaviour in condition number with the conventional polynomial model.

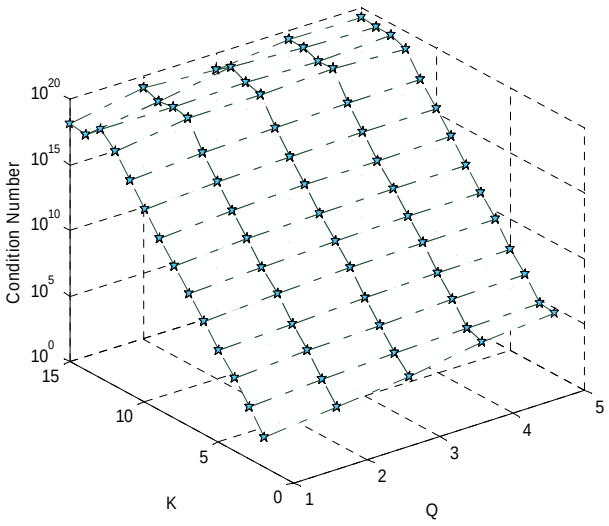

Fig. 4. Condition number of the $(\Phi^H\Phi)$ matrix, when K order of nonlinearity and Q delay tap is used in basis function conventional polynomial model (K = 15,Q = 4).

It has been shown that the orthogonal polynomial condition number is lower than the conventional polynomial one in both memory-less and memory cases. We observe that the condition number increases exponentially as a function of the nonlinearity order K, and the memory depth Q and becomes large even for a moderate K and Q. This implies that, in practise, the inversion of $(\Phi^H\Phi)$ can be difficult than $(\Psi^H\Psi)$. Fig. 5 shows the condition number for the matrix $(\Psi^H\Psi)$ for 3000 samples. We note that, the condition number increases at a much slower rate as K and Q increases. A low condition number will ensure better numerical stability when finite precision computation of the model coefficients is needed. We have carried out from the analysis of the condition numbers in fig.4 and fig. 5, to show that the orthogonal polynomial basis is advantageous to the envelope memory polynomial model and the conventional polynomial model. We note that the envelope memory polynomial model and the conventional polynomial one have almost the same behavior. The delay alignment between the input and output data is a significant constraint, therefore, if it is not perfectly cancelled. The delay alignment causes additional dispersion in the AM/AM and AM/PM characteristics of the Power Amplifier (PA) and carries out inaccurate behavioural modelling performances.

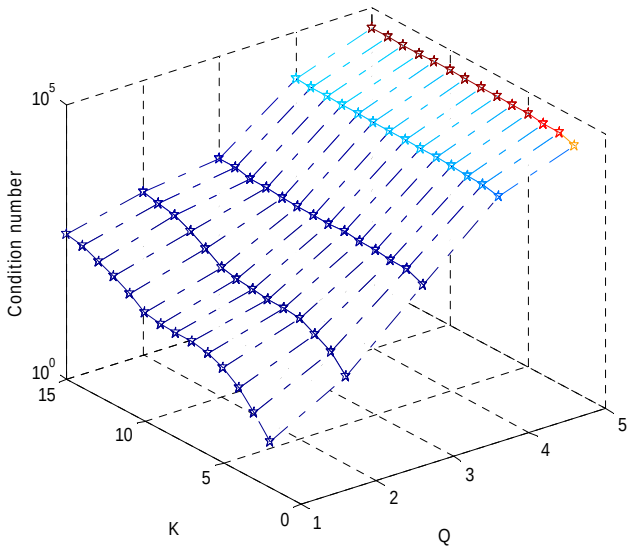

Fig. 5. Condition number of the $(\Psi^H\Psi)$ matrix, when K order of nonlinearity and Q delay tap is used in basis function orthogonal polynomial model (K = 15,Q = 4).

This delay is mainly due to the sampling rate of the input and output waveforms, which is limited by the available ADC speed. Indeed, an up-sampling ratio is needed to accurately estimate the delay between the input and output data, such a solution for this problem.

For this test-bed measurement in fig.2-3, the actual output sample depends only on the actual input sample. The delay alignment sensitivity for our input output QPSK signal is shown in fig. 6, where the measure and the model are not synchronous ant the shift is caused by the delay alignment between the input and output data.

Fig.7 and fig.8 shows a comparison between the Polynomial Model, envelope memory polynomial model, the orthogonal polynomial model and the measurements after cancelling the delay between the input and the output of the power amplifier. In fig.7, the temporal waveform is plotted (the output versus samples), however, fig.8 shows the QPSK constellation (Q versus I) for the models and the measurements.

The delay alignment influence causes a degradation of the Behavioural model performance, whilst, this delay can be considered as kind of the memory effects for one memory effects system consideration.

First, a simulation sweep on the DUT nonlinearity order and memory depth was performed for both the EMPM and OMPM models. For each combination of the model parameters the NMSE between the estimated model output and the measured data was calculated.

To examine the goodness of fit of a Polynomial Power amplifier PA, when we assume 3000 PA input and output samples are used, we calculated the modelled power amplifier output according to (2) and the corresponding NMSE according to (11).

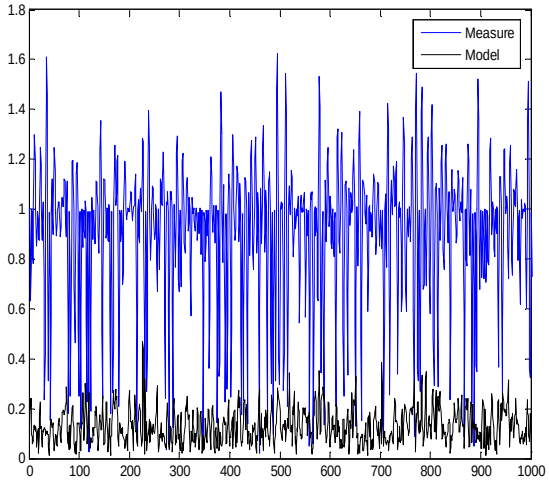

Fig.6. Measure and model output waveform before deleting the delay alignments between the input and output data

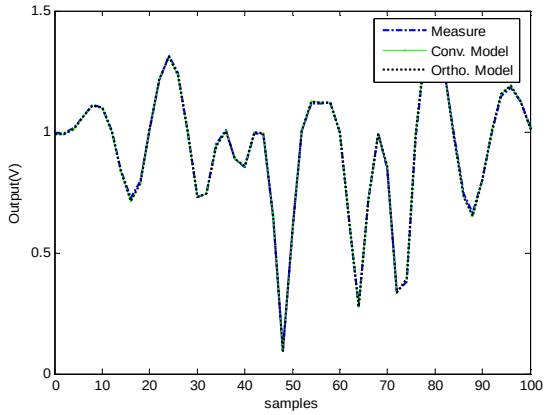

Fig.7. Measured and modelled output waveform after deleting the delay alignment between the input and output data

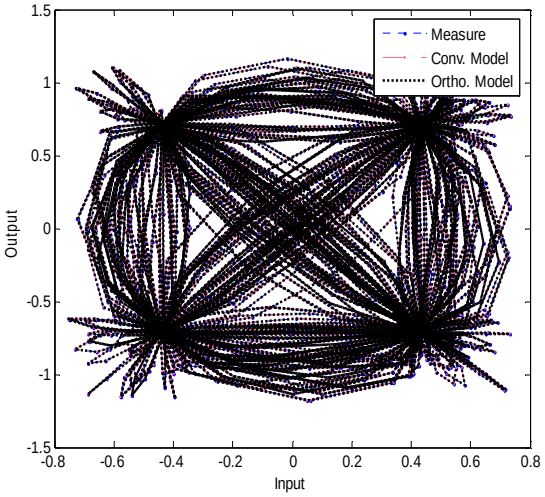

Fig.8. Measured and modelled output constellation QPSK without delay alignments between the input and output data

Fig.9, shows the NMSE when the conventional and orthogonal basis functions are used. The general trend is that the NMSE first decreases with increasing polynomial nonlinearity order K from one hand, and increasing polynomial memory depth Q in other hand. After a threshold of a nonlinearity order K, we note that the NMSE is almost constant around -40dB. As soon as, the delay tap Q increases with the same nonlinearity order as previous, the NMSE decreases to reach a significant value compared to the memory-less conventional polynomial case(Q = 2).

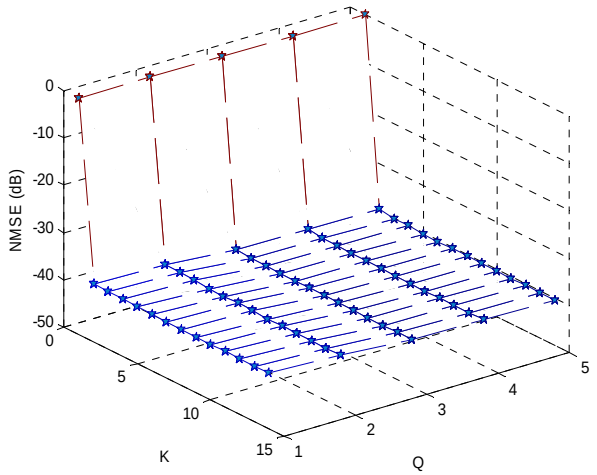

Fig.9. Polynomial PA modelling errors when K conventional and orthogonal polynomial order basis functions and Q delay tap are used (K = 15,Q = 4).

To study the robustness of the experimental setup measurement testbed fig.1-2, when it is applied to a nonlinear power amplifier (PA) biased in class AB operation which is built using MESFET transistor (Fujitsu FLL107ME) and operates around 1575 MHz. This amplifier is characterized under a QPSK signal excitation with a chip rate of 1 Msps. Fig.9, shows the AM/PM characteristics of the measure, the conventional polynomial model, the envelope memory polynomial model and the orthogonal polynomial model. It has shown that the power amplifier exhibits an important nonlinear characteristics explained by its shape. The AM/PM curve shows a little dispersion due to static nonlinearity and weak memory effect. The memory effect attributed mainly to the non-constant frequency response around the carrier frequency, the impedance variation of the bias circuits and the harmonic loading of the power transistors.

The existence of the distortions created by nonlinearity of power transistors and the objective of its reduction carry out to apply the memory-less base-band pre-distortion as a linearization technique, which is applied in a load-pull/source-pull measurement system [16].

The input signal bandwidth influences the power amplifiers behaviour through memory effects. We talked about two kind of memory such as thermal and electrical memory effects. Therefore, when power amplifiers are

driven under narrow band input signals, we find heating effects that occur at the junction level. Different frequency ranges for the thermal memory effects, where, the time constant is closed between [10us, 1ms].
For wideband signals, electrical memory effects are predominant and are mainly due to the frequency response of the bias circuit over the modulation bandwidth of the input signal.
The effects can be minimized by appropriate design of the bias network. However, they are observed for bandwidth exceeding 10MHz.
Since WCDMA signal having 5MHz bandwidth per carrier, the thermal memory effects, are not observed in the behaviour of the device under test. When multi-carrier WCDMA signals are used, the resulting bandwidth emulates the electrical memory effects in the behaviour of the power amplifier. These electrical memory effects appear as dispersion in the measured characteristics of the PA.

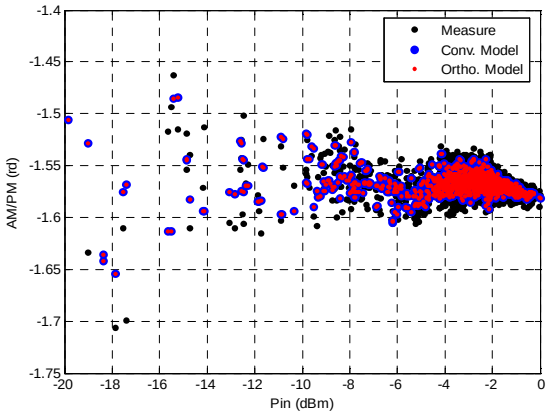

Fig.10. AM/PM characteristic of the power amplifier, using MESFET transistor measure, and models.

It has been taken that any nonlinearity in the transfer characteristic of a power amplifier constitutes a problem of some kind, but no attempts have been made to quantify the problem. In cases in which the modulation system varies the amplitude, it would seem to be a logical extension, or application of these P_{in} - P_{out} transfer characteristic to map the input amplitude variations onto the output plane. This resulting distorted waveform can then be analyzed for its frequency components, which constitute the spectral distortion caused by the amplitude nonlinearity of the amplifier. Any amplifier, when driven into a strongly nonlinear condition, will exhibit phase as well as amplitude distortion. This usually, is characterized in terms of AM-PM conversion, and represent a change in the phase of the transfer characteristic as the derive level is increased toward and beyond the compression point. It will be seen that AM-PM in typical solid state amplifiers is a significant, but rarely a dominant effect. The usefulness and validity of results that ignore AM-PM are substantial. The most common manifestation of AM-PM effects is an irritating asymmetrical slewing of the intermodulation (IM) or spectral regrowth display. The precise cause of this effect is the key to understanding and quantifying the importance of AM-PM effects in individual cases.
The power series is trotted as a generalized formulation for non linear behaviour, but it clearly has some limitations, there is no phase component in the linear output term. Therefore, the output would show both amplitude and phase changes from the input signal. The use of power series is limited additionally by the problem that a_n coefficient are sensitive (not constant) to change in the input and output tuning and to the bias levels at input and output. Power amplifiers operating at or beyond the compression require different treatment because the nonlinearities become strong and arise through the cutoff and clipping behaviour of the transistor. Strongly nonlinear effects refer to the distortion of the signal waveform that is caused by the limiting behaviour of the transistor. It is instructive to attempt to model the PA, because we see the difference between strong and weak nonlinear effects and experience the difficulty to satisfying both with the same model.
The coefficients of power amplifier model would be more variable (not constant) with bias point but the negative sign shows that limiting action will occur and serves to model the saturation of the device as hard saturation is approached.

V. CONCLUSION

In this work, an experimental setup measurement test bed for the characterization of nonlinear RF power amplifier is presented. The measurement system is mainly devoted to mimic a robust power amplifier model. In order to deduce the identification of a conventional Polynomial model, the envelope memory polynomial model and the orthogonal polynomial model resulting in memory-less AM/AM and AM/PM characteristics were utilized to de-embed the raw measurement data. To characterize the power amplifier with a Polynomial model accurately, a time delay estimation and cross-covariance calculation was used to align the input and output raw baseband data which captured beforehand. Indeed, to evaluate the accuracy and robustness of the Conventional Polynomial model, a simple method of baseband memory-less pre-distortion was presented and implemented in a load-pull system [16]. Therefore, to take account of the memory effects for the pre-distortion improvements, an application under development in our future work.

REFERENCES

1. P. B. Kenington,"High Linearity RF Amplifier Design,"Artech House 2000.
2. S. M. McBeath, D. T. Pinckley, J. R. Cruz,"W-CDMA power amplifier modelling," Vehicular Technology ConferenceVTC. 54th, 2001 pp 2243-2247.
3. D. Giesber, S. Mann, K. Eccleston,"Adaptive Digital Predistortion Linearization for RF Power Amplifiers," Proceedings of the 13th Electronics New Zealand Conference Nov.2006.
4. A. Zhu, T. J. Brazil,"An Overview of Volterra Series Based Behavioral Modeling of RF/Microwave Power Amplifiers,"Wireless and Microwave Technology Conf., Dec.2006
5. S. J. Orfanidis, "Optimum Signal Processing: An introduction," 2nd Edition, Prentice-Hall, 1996.
6. E. Bergeault, O. Gibrat, S. Bensmida, and B. Huyart," Multiharmonic source-pull/load-pull active setup based on six-port reflectometers: Influence of the second harmonic source impedance on RF performances of power transistors," IEEE Trans. Microw. Theory Tech. vol. 52, no.4, pp1118-1124, Apr. 2004.
7. J. P. Aikio, and T. Rahkonen,"A comprehensive analysis of AM/AM and AM/PM conversion in an LDMOS RF power amplifier," IEEE Trans. Microw. Theory Tech. vol. 57, no.2, pp262-270, Feb. 2009.
8. D. J. Williams, J. Leckey, and P.J. Tasker," Envelope domain analysis of measured time domain voltage and current waveforms provide for improved understanding of factors effecting linearity," in IEEE MTT-S Int. Microw. Symp. Dig., Jun. 2003, pp.1411-1414.
9. S. Y. Lee, Y. S. Lee, S. H. Hong, H. S. Choi, and Y. H. Jeong,"An adaptive predistortion RF power amplifier with a spectrum monitor for multicarrier WCDMA applications," IEEE Trans. Microw. Theory Tech. vol. 53, no.2, pp 786-793, Feb. 2005.
10. L. Ding, G. T. Zhou, D. R. Morgan, Z. Ma, J. S. Kenney, J. Kim, and C. R. Giardina," A robust digital baseband predistorter constructed using memory polynomials," IEEE Trans. Commun.vol.52, no. 1, pp 159-165, Jun. 2004.
11. Raich, R., Q. Hua, and G.T. Zhou, Orthogonal polynomials for power amplifier modeling and predistorter design. Vehicular Technology, IEEE Transactions on, 2004, p. 1468-1479.
12. C. Fager, J. C. Pedro, N. B. De carvalho, and H. Zirath," Prediction of IMD in LDMOS transistor amplifiers using a new large signal model," IEEE Trans. Microw. Theory Tech., vol. 50, no. 12, pp. 2834-2842, Dec. 2002.
13. Y. S. Jeon, J. Cha. and S. Nam," High efficiency power amplifier using novel dynamic bias switching," IEEE Trans. Microw. Theory Tech. vol. 55, no.4, pp690-696, Apr. 2007.
14. S. L. Miller, and R. J. O'Dea,"Peak power and bandwidth efficient linear modulation," IEEE Trans. Commun. vol. 46, no.12, pp 1639-1648, Dec. 1998.
15. S. Mahil, and A. B. Sesay," Rational function based predistorter for traveling wave tube amplifiers," IEEE Trans. On Broadcast. Vol. 51, no. 1, Mar. 2005
16. C.Peng, W. Jiang, Y. Ni, J. Wang, X. Yu, B. Xing, X. Zhu,"Modeling of nonlinear power amplifier with memory effects applied for 3G system," Microwave Conference Proceedings, APMC, Asia-Pacific, Dec.2005.
17. S. Bensmida, E. Bergeault, G. I. Abib, and B. Huyart," Power amplifier characterization: An activeload-pull system based on six port," IEEE Trans. Microw. Theory Tech., vol.54,no.6, pp2707-2712, Jun. 2006.